Bioorganic & Medicinal Chemistry Letters 21 (2011) 7367–7372

Contents lists available at SciVerse ScienceDirect

Bioorganic & Medicinal Chemistry Letters

journal homepage: www.elsevier.com/locate/bmcl

2,6-Naphthyridines as potent and selective inhibitors of the novel protein kinase C isozymes

Maurice J. van Eis [a,*], Jean-Pierre Evenou [a], Philipp Floersheim [a], Christoph Gaul [a], Sandra W. Cowan-Jacob [a], Lauren Monovich [b], Gabriele Rummel [a], Walter Schuler [a], Wilhelm Stark [a], Andre Strauss [a], Anette von Matt [a], Eric Vangrevelinghe [a], Juergen Wagner [a], Nicolas Soldermann [a]

[a] Novartis Institutes for BioMedical Research, Forum 1, Novartis Campus, CH-4056 Basel, Switzerland
[b] Novartis Institutes for BioMedical Research, 100 Technology Square, Cambridge, MA 02139, USA

ARTICLE INFO

Article history:
Received 7 July 2011
Revised 5 October 2011
Accepted 7 October 2011
Available online 21 October 2011

Keywords:
Protein Kinase C
Inhibitors
Isozyme specific
2,6-Naphthyridines
T cell inhibition

ABSTRACT

The present study describes a novel series of ATP-competitive PKC inhibitors based on the 2,6-naphthyridine template. Example compounds potently inhibit the novel Protein Kinase C (PKC) isotypes δ, ε, η, θ (in particular PKCε/η, and display a 10–100-fold selectivity over the classical PKC isotypes. The prototype compound **11** was found to inhibit PKCθ-dependent pathways in vitro and in vivo. In vitro, a-CD3/a-CD28-induced lymphocyte proliferation could be effectively blocked in 10% rat whole blood. In mice, **11** dose-dependently inhibited *Staphylococcus aureus* enterotoxin B-triggered IL-2 serum levels after oral dosing.

Protein kinase C (PKC) comprises a family of 11 serine/threonine kinases which can be grouped into three subfamilies based on the different co-factors required for optimal catalytic activity. The classical isotypes, PKCα/β/γ require the second messengers diacylglycerol (DAG) and Ca^{2+} for their activation, whereas the novel isotypes PKCδ/ε/η/θ only require DAG. In contrast, the atypical isotypes PKCι/λ/ξ do not require Ca^{2+} or DAG to be able to exert their full catalytic activity. Multiple members of the PKC family play a central role in the signaling cascades of the immune system, the key players being the classical PKC isotypes δε and the novel PKC isotype θ.[1] In particular for PKCθ a crucial role in T cell receptor (TCR)–mediated T cell activation and proliferation has been established.[2] The different PKC isotypes and especially PKCθ, are therefore considered to be attractive therapeutic targets for the treatment of autoimmune diseases and transplantation. However, to date only Sotrastaurin (AEB071), a potent nanomolar ATP-competitive inhibitor of all classical and novel PKC isotypes[3a,b] has progressed to clinical trials as a potential treatment of psoriasis[3c] and for the prevention of allograft rejection following renal transplantation.[3d,e] Given the crucial role of PKCθ in T cell activation/proliferation, many groups have initiated drug discovery programs aiming at the development of PKCθ selective compounds. Recently progress was reported towards selective ATP-competitive PKCθ inhibitors based on the thieno[2,3-*b*]pyridine-5-carbonitrile[4a–g] and 2,4-diamino-5-nitropyrimidine scaffolds.[4h]

Surprisingly, inhibitors displaying selectivity for the novel PKC isotype family (δεηθ) over the classical isotypes (δε) have not been reported, despite the close relationship between these isotypes in the phylogenetic tree. In this communication we report the first examples of low molecular weight compounds displaying such a selectivity profile. These compounds showed promising cellular activity and have attractive biopharmaceutical properties.

In a search for PKCθ inhibiting chemotypes, a high-throughput docking (HTD) screen was performed. Docking[5] of the Novartis compound archive into the ATP binding site of PKCθ using the X-ray crystal structure of PKCθ (PDB code 1XJD)[6] and subsequent profiling of the 641 highest ranked hits against a panel consisting of six PKC isotypes led to the identification of compound **1** as a potent inhibitor of PKCθ. In addition to inhibition of PKCθ, **1** also potently inhibits the novel PKC isotypes δε, η whilst displaying an excellent selectivity over the classical PKC isotypes δε (see Table 1).

In the binding mode identified by HTD, **1** engages in a single canonical H-bond to Leu 461 located in the hinge region of the ATP binding site of PKCθ with the 4-pyridyl moiety serving as a H-bond acceptor. In addition, the nitrogen atom in the 6-position of the naphthyridine core is predicted to make a H-bond to the catalytic lysine residue Lys 409. An alternative binding mode in which the pyridyl ring and the naphthyridine ring switch positions

* Corresponding author. Tel.: +41 61 3248293; fax: +41 61 3246735.
E-mail address: maurice.van_eis@novartis.com (M.J. van Eis).

0960-894X/$ - see front matter © 2011 Elsevier Ltd. All rights reserved.
doi:10.1016/j.bmcl.2011.10.025

Table 1
IC_{50} values of isoquinoline and naphthyridine based PKC inhibitors against a panel of PKC isotypes (IC_{50} values in nM)[ab]

Compound	R	α	β1	δ	ε	η	θ
1	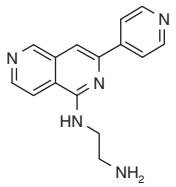	900	859	20	5	5	77
2	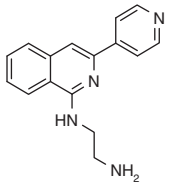	>1000	>1000	>1000	877	743	>1000
3	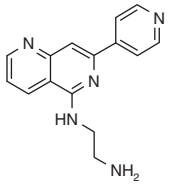	>1000	>1000	>1000	929	401	> 1000
4	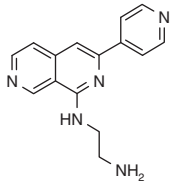	>1000	>1000	>1000	>1000	>1000	>1000
5	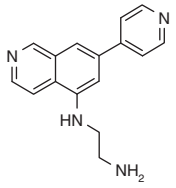	>1000	>1000	157	44	54	355
6	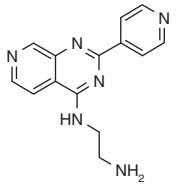	>1000	>1000	102	38	27	>1000

[a] Mean values of at least two independent measurements.
[b] Scintillation Proximity Assay (SPA), see Refs. 3a,b,7a,b.

resulting in H-bond formation between the nitrogen atom in the 6-position of the naphthyridine core and the hinge of the kinase seemed plausible as well. In order to test our binding mode hypothesis, a series of naphthyridine derivatives were synthesized (compounds **2–6**, see Table 1). The N→CH replacement in the 6-position of the naphthyridine core (compound **2**) led to a 100 fold drop in binding affinity to all PKC isotypes. Interestingly, some modest binding affinity to PKCεη was retained suggesting that the naphthyridine core is not involved in binding to the hinge. As anticipated from the binding model, shifting of the nitrogen atom into the 5-position (compound **3**) did not improve inhibitory activity on the different PKC isotypes. All PKC inhibitory activity was lost with the 7-aza-analogue **4**. Removal of the nitrogen atom in the 2-position of the naphthyridine core of **1** (compound **5**) led to a 10-fold loss of binding affinity to PKCεη and ablation of inhibitory activity on PKCθ. We speculate that for optimal binding affinity the pyridyl ring and the naphthyridine ring need to be co-planar. The N→CH modification may have a detrimental steric effect on the required co-planarity of the pyridyl and isoquinoline rings. However, introduction of an additional nitrogen atom into the 4-position of the naphthyridine core (compound **6**) with the aim of further favouring the co-planarity of the two aromatic rings did not have a positive impact on the binding affinity. Although inhibitory potency on PKCεη was retained, binding affinity to PKCθ was ablated.

Compound **1** and the majority of the compounds listed in this paper could be synthesized by adapting the synthetic protocols previously reported by Meredith et al. for similar compounds, using the appropriate starting materials.[8]

For some compounds an alternative synthesis was used (**12**, **23** and **24**). This is exemplified in Scheme 1 for compound **12**.

Starting from the commercially available 3-methyl-pyridine-N-oxide (**7**) the 3-methyl-isonicotinonitrile (**8**) could be obtained in gram amounts. Deprotonation of **8** with sodium hydride and subsequent reaction with isonicotinic acid methyl ester afforded **9**. We accidentally discovered that **9** was unstable under column

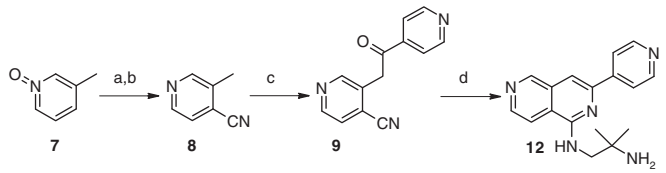

Scheme 1. Reagents and conditions: (a) Dimethyl sulfate (1.1 equiv), 40 °C, 16 h; (b) KCN (1.1 equiv), EtOH/H_2O (1:1), 40 °C, 16 h, 34%; (c) NaH (4.0 equiv), isonicotinic acid methyl ester (1.0 equiv), DME, 95 °C, 16 h., 100%; (d) 2-methyl-propane-1,2-diamine (10 equiv), EtOAc/acetic acid (6:4), Silica Gel 60 (15 weight equiv), rt, 2 h, 47%.

chromatography conditions and that cyclisation gave rise to a naphthyridinone. When **9** was stirred in a mixture of ethyl acetate and acetic acid in the presence of silica gel and an excess of 2-methyl-propane-1,2-diamine, **12** could be isolated in 47% yield. The scope and limitations of this reaction as well the proposed mechanism will be the subject of a separate paper.

In a second round of optimization, the SAR around the basic amine-containing side chain was explored. A summary of the data is given in Table 2. Replacement of the nitrogen linker by an oxygen linker led to an approximately 20-fold loss in binding affinity to the novel PKC isotypes (**10**). The introduction of a small lipophilic substituent at the δ-carbon to the basic amine further improved binding affinity to the novel PKC isotypes (**11**). The corresponding (*R*)-enantiomer of **11** (structure not shown) was around 10-fold less potent on all PKC isotypes. In line with this, gem-dimethyl substitution (**12**) did not further improve potency. Likewise, the introduction of large lypophilic substituents (**13**) was poorly tolerated. Alkylation of the linker nitrogen atom or the basic amine led to a 5- and 20-fold drop in binding affinity

Table 2
Variations around the flexible side-chain of **1** (IC_{50} values in nM)[ab]

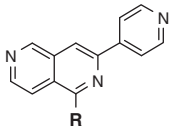

Compound	R	α	β1	δ	ε	η	θ
10	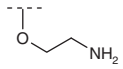	>1000	>1000	703	120	82	948
11	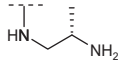	829	378	8	5	2	55
12	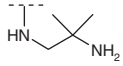	967	942	44	18	9	141
13	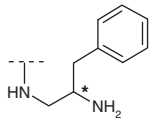	818	>1000	932	403	452	>1000
14	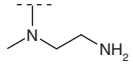	>1000	>1000	371	24	34	350
15	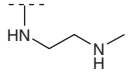	>1000	>1000	254	79	93	997
16	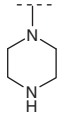	>1000	823	31	8	6	109
17	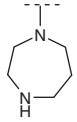	433	661	63	7	4	77
18	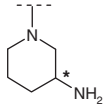	771	865	214	8	13	132
19	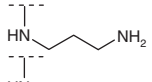	676	779	53	13	10	97
20	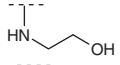	>1000	>1000	635	81	188	743
21	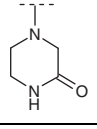	>1000	>1000	>1000	802	735	>1000

[a] Mean values of at least two independent measurements.
[b] Scintillation Proximity Assay (SPA), see Refs. 3a,b,7a,b.

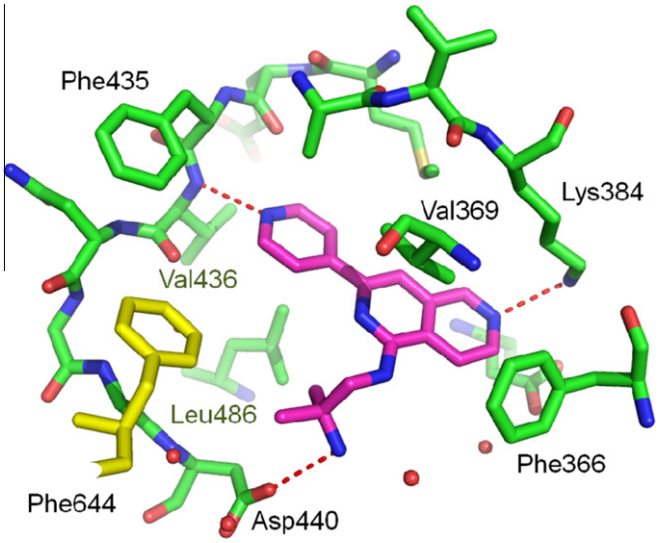

Figure 1. X-ray crystal structure of **12** (green)η (carbons in magenta) bound to the ATP-binding site of PKC[9] solved at 2.05 Å resolution. Hydrogen bonds are indicated by dashed red lines and water molecules by red spheres.

(**14** and **15**, respectively). Binding affinity was retained when the linker nitrogen atom or the basic amine were incorporated into a cyclic fragment (**16**, **17** and **18**). A chain length of two carbon atoms proved to be ideal. A three-carbon spacer (**19**) was tolerated but longer chain lengths were unfavourable. The basic amine proved to be essential for achieving a high binding affinity to the novel PKC isozymes which is in line with the binding hypothesis suggesting the occurrence of a salt bridge between an aspartate residue of the protein and the protonated amine. Substitution of the amine by a hydroxyl group (**20**) strongly attenuated binding affinity whereas an amide group ablated binding affinity (**21**).

Table 4
Inhibition of a-CD3/aCD28 induced rat T lymphocyte proliferation[a,b,c]

Compound	**5**	**12**	**11**
IC_{50}	1041	356	138

[a] Mean values of at least two independent measurements.
[b] See Ref. 11.
[c] Assay run in the presence of 10% rat blood.

We were not able to obtain an X-ray crystal structure of one of the naphthyridines bound to PKCθ. However, we did obtain an X-ray crystal structure of **12** bound to the kinase domain of PKCη (see Fig. 1).[9] PKCη adopts an active conformation despite the fact that tyrosine 513 in the activation loop is non-phosphorylated. The X-ray crystal structure unambiguously demonstrates that **12** adopts the binding mode found by HTD in which the pyridyl moiety makes a single hydrogen bond to the hinge region of the protein (Val 436). This binding mode is identical to the recently proposed binding mode of similar compounds to Protein Kinase D.[8] No indication was found for the occurrence of an alternative binding mode in which the key interaction to the hinge would involve the naphthyridine core as it has been already hypothesized for other naphtyridine-based inhibitors targeting SYK[10a] and CK2[10b] kinases. The nitrogen in the 6-position of the naphthyridine core is involved in hydrogen bonding to the catalytic lysine residue (Lys 384) whereas the basic amine forms a salt bridge to Asp 440 located in the sugar pocket. The inhibitor is tightly packed in the ATP binding pocket and strong lipophilic interactions occur between Leu 486 and the pyridyl ring and Val 369 and the naphthyridine core. In addition a strong face-to-edge interaction occurs between the naphthyridine ring and a phenyl alanine residue (Phe 366) situated in the P-loop.

The X-ray crystal structure does not provide a satisfactory explanation for the observed PKC isotype selectivity. Of all the residues of the protein which make a direct contact with the inhibitor

Table 3
Variations around pyridyl ring of **12** (IC_{50} values in nM)[a]

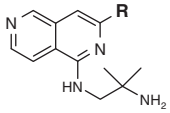

Compound	R	α	β1	δ	ε	η	θ
22		>1000	>1000	>1000	>1000	>1000	>1000
23	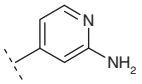	378	>1000	294	147	60	496
24	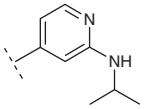	>1000	>1000	>1000	>1000	862	>1000
25	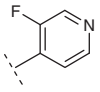	>1000	961	124	62	18	140
26	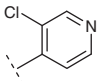	>1000	>1000	221	47	15	93
27	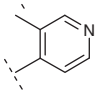	>1000	>1000	386	133	52	738

[a] Mean values of at least two independent measurements.
[b] Scintillation Proximity Assay (SPA), see Refs. 3a,b,7a,b.

Table 5
Pharmacokinetic properties of **11** in rats and efficacy in a mouse SEB model[a,b]

Intravenous (iv) dose = 5 mg /kg		Oral (po) dose = 10 mg /kg		Mouse SEB model[b] inhibition [%] ± standard deviation		
AUC_{∞} (ng h mL^{-1})	1770	AUC_{∞} (ng h mL^{-1})	712	50 mg/kg	37 ± 25	$p = 1.6 \times 10^{-2}$
$t_{½\ E}$ (h)	8.1	T_{max} (h)	2.0	100 mg/kg	70 ± 15	$p = 3 \times 10^{-4}$
Cl (mL min^{-1} kg^{-1})	49	C_{max} (ng/mL)	53			
V_{ss} (L/kg)	14.0	F(%)	20			

[a] Data reported as the average of three animals (Lewis rats). Vehicle for iv: 85% water–15% PEG200. Vehicle for po: 92.5% water/HCl (pH 4) – 7.5% PEG200. AUC_{∞}: Area under the curve extrapolated to infinity.
[b] SEB model, see Refs. 16,17.

only one difference exists between the novel and classical PKC isotypes (Leu 486 (PKCη, see Fig. 1) → Met 470 (PKCδ)). We feel that this difference is insufficient to rationalize the observed isotype selectivity. We speculate that the origin of the observed isotype selectivity may reside in a difference in the flexibility of the P-loop between the different isotypes. A more flexible P-loop in the novel PKC isotypes may allow for more favourable van der Waals contacts between the protein and the inhibitor.

In another round of optimisation, the SAR around the hinge binding pyridyl moiety was investigated (see Table 3). Changing the connectivity of the naphthyridine core to the pyridyl fragment (**22**) was not tolerated, which is in line with the observed binding mode. Adding a hydrogen bond donor to the 2-position of the pyridyl ring, with the potential to make an additional hydrogen bond to the hinge region of the protein, reduced binding affinity (**23**). Larger substituents in the 2-position (**24**) fully ablated binding affinity. Halogen atoms in the 3-position of the pyridyl ring were tolerated (**25**/**26**) but did not have a favourable impact on the binding affinity whereas a methyl group had a detrimental effect (**27**).

A number of derivatives were tested for their ability to inhibit anti-CD3/anti-CD28 induced proliferation of rat T-lymphocytes in 10% whole blood.[11] This assay is expected to be PKCθ-dependent as this isoform integrates signaling pathways downstream of the T cell receptor and the CD28 co-receptor. The role of the other novel PKC isoforms in T cell activation is not well understood. Indeed inhibition of the novel PKC isotypes translated into inhibition in the proliferation assay. The limited data set suggests that the IC_{50} values for inhibition in the proliferation assay track the inhibition of PKCθ in the biochemical assay (see Table 4).

Compound **11** showed good activity in the proliferation assay (IC_{50} = 138 nM) and was selected for further profiling against a panel of 224 human serine/threonine and tyrosine protein kinases.[12] Compound **11** shows a promising kinase selectivity with only 38 kinases inhibited by more than 50% and only 16 kinases (including the novel PKC isotypes) inhibited by more than 80% at a compound concentration of 1 μM. Among the kinases which were strongly inhibited in addition to the novel PKC isotypes are closely related AGC kinases such as PKA, PKD, PKN-1, -2 and ROCK-1, 2.

Compound **11** possesses attractive ADMET properties. The compound combines a good intrinsic aqueous solubility (>0.4 g/L) with a medium permeability.[13] The primary amine of **11** is strongly basic (pK_a = 9.0) which results in a large difference between log$P$ (2.2) and $logD_{6.8}$ (−0.3). As a consequence of the low lipophilicity of **11**, the degree of binding to human and rat plasma proteins is low (58 and 63%, respectively).[14] Cytochrome P450 inhibition was only observed for CYP1A2 with an IC_{50} value of 2.4 μM. The potential of **11** to interact with the hERG (human Ether-a-go-go Related Gene) channel was assessed in a radioligand (dofetilide) binding assay.[15] Surprisingly, **11** did not inhibit the hERG channel (IC_{50} >30 μM), despite the fact that the compound contains the typical hERG pharmacophoric features consisting of two aromatic rings in combination with a strongly basic amine.

The in vivo pharmacokinetic parameters of **11** in rats are summarised in Table 5 and are in line with its physico-chemical properties. The iv pharmacokinetic profile of **11** is characterised by a large volume of distribution which is typical for a strongly basic compound. Clearance is medium high, resulting in an elimination half-life of 8.1 h. The po pharmacokinetic profile is characterised by a relatively rapid absorption which is in line with the good aqueous solubility and medium permeability of **11**. Oral bioavailability is modest (20%).

Compound **11** was subsequently tested in vivo using the model of SEB-induced IL-2 production in BALB/c mice.[16,17] In this experiment, **11** showed dose-dependent, statistically significant inhibition of SEB-triggered release of IL-2. At an oral dose of 100 mg/kg 70% inhibition was achieved whereas inhibition was 37% at the lower dose of 50 mg/kg.

In summary, we have reported the first examples of a new class of PKC inhibitors based on the 2,6-naphthyridine scaffold which show high selectivity for the novel over the classical PKC isotypes. Selected derivatives show activity in a PKCθ dependent cellular assay and have attractive biopharmaceutical properties. For the prototype compound **11** this translated into promising inhibition of IL-2 release in vivo after SEB stimulation. We believe that these compounds may also serve as tool compounds to further dissect the role of the different PKC isotypes in signaling pathways. Efforts are ongoing to further improve the binding affinity of these compounds to PKCθ.

Acknowledgment

Christoph Burkhart is kindly acknowledged for performing the mouse SEB experiments.

Supplementary data

Supplementary data associated with this article can be found, in the online version, at doi:10.1016/j.bmcl.2011.10.025.

References and notes

1. For reviews, see: (a) Baier, G.; Wagner, J. *Curr. Opin. Cell Biol.* **2009**, *21*, 262; (b) Roffey, J.; Rosse, C.; Linch, M.; Hibbert, A.; McDonald, N. C.; Parker, P. J. *Curr. Opin. Cell Biol.* **2009**, *21*, 268; (c) Lee, M. R.; Duan, W.; Tan, S. *Expert Opin. Ther. Targets* **2008**, *12*, 535; (d) Hayashi, K.; Altman, A. *Pharm. Res.* **2007**, *55*, 537; (e) Chaudhary, D.; Kasaian, M. *Curr. Opin. Invest. Drugs* **2006**, *7*, 432; (f) Thuille, N.; Gruber, T.; Pfeifhofer, C.; Hermann-Kleiter, N.; Lutz-Nicoladoni, C.; Letschka, T.; Kollmann, V.; Leitges, M.; Baire, G. *Curr. Immmunol. Rev.* **2006**, *2*, 143.
2. (a) Kingeter, L. M.; Schaefer, B. C. *J. Immunol.* **2008**, *181*, 6244; (b) Manicassamy, S.; Gupta, S.; Sun, Z. *Cell. Mol. Immunol.* **2006**, *3*, 263; (c) Pfeifhofer, C.; Kofler, K.; Gruber, T.; Tabrizi, N. G.; Lutz, C.; Maly, K.; Leitges, M.; Baier, G. *J. Exp. Med.* **2003**, *197*, 1525; (d) Sun, Z.; Arendt, C. W.; Ellmeier, W.; Schaeffer, E. M.; Sunshine, M. J.; Ghandi, L.; Annes, J.; Petrzilka, D.; Kupfer, A.; Schwartzberg, P. L.; Littman, D. R. *Nature* **2000**, *404*, 402.
3. (a) Wagner, J.; Von Matt, P.; Sedrani, R.; Albert, R.; Cooke, N.; Ehrhardt, C.; Geiser, M.; Rummel, G.; Stark, W.; Strauss, A.; Cowan-Jacob, S. W.; Beerli, C.; Weckbecker, G.; Evenou, J.-P.; Zenke, G.; Cottens, S. *J. Med. Chem.* **2009**, *52*, 6193; (b) Evenou, J.-P.; Wagner, J.; Zenke, G.; Brinkmann, V.; Wagner, K.; Kovarik, J.; Welzenbach, K. A.; Weitz-Schmidt, G.; Guntermann, C.; Towbin, H.; Cottens, S.; Kaminski, S.; Letschka, T.; Lutz-Nicoladoni, C.; Gruber, T.; Hermann-Kleiter, N.; Thuille, N.; Baier, G. *J. Pharm. Exp. Ther.* **2009**, *330*, 792; (c) Skvara, H.; Dawid, M.; Kleyn, E.; Wolff, B.; Meingassner, J. G.; Knight, H.; Dumortier, T.; Kopp, T.; Fallahi, N.; Stary, G.; Burkhart, C.; Grenet, O.; Wagner, J.; Hijazi, Y.;

Morris, R. E.; McGeown, C.; Rordorf, C.; Griffiths, C. E. M.; Stingl, G.; Jung, T. *J. Clin. Invest.* **2008**, *118*, 3151; (d) Matz, M.; Naik, M.; Mashreghi, M.-F.; Glander, P.; Neumayer, H.-H.; Budde, K. *Expert Opin. Drug Metab. Toxicol.* **2011**, *7*(1), 103; (e) Sommerer, C.; Zeier, M. *Clin. Transplant.* **2009**, *23*, 15.

4. (a) Boschelli, D. H.; Subrath, J.; Niu, C.; Wu, B.; Wang, Y.; Lee, J.; Brennan, A.; Ho, M.; Deng, B.; Yang, X.; Xu, X.; Leung, L.; Wang, J.; Atherton, J.; Chaudhary, D. *Bioorg. Med Chem.* **2010**, *20*, 1965; (b) Tumey, L. N.; Bhagirath, N.; Brennan, A.; Brooijmans, N.; Lee, J.; Yang, X.; Boschelli, D. H. *Bioorg. Med Chem.* **2009**, *19*, 7933; (c) Shim, J.; Eid, C.; Lee, J.; Liu, E.; Chaudhary, D.; Boschelli, D. H. *Bioorg. Med. Chem. Lett.* **2009**, *19*, 6575; (d) Niu, C.; Boschelli, D. H.; Tumey, L. N.; Bhagirath, N.; Subrath, J.; Shim, J.; Wang, Y.; Wu, B.; Eid, C.; Lee, J.; Yang, X.; Brennan, A.; Chaudhary, D. *Bioorg. Med. Chem. Lett.* **2009**, *19*, 5829; (e) Boschelli, D. H.; Wang, D.; Prashad, A. S.; Subrath, J.; Wu, B.; Niu, C.; Lee, J.; Yang, X.; Brennan, A.; Chaudhary, D. *Bioorg. Med. Chem. Lett.* **2009**, *19*, 3623; (f) Wu, B.; Boschelli, D. H.; Lee, J.; Yang, X.; Chaudhary, D. *Bioorg. Med. Chem. Lett.* **2009**, *19*, 766; (g) Cole, D. C.; Asselin, M.; Brennan, A.; Czerwinski, R.; Ellingboe, J. W.; Fitz, L.; Greco, R.; Huang, X.; Joseph-McCarthy, D.; Kelly, M. F.; Kirisits, M.; Lee, J.; Li, Y.; Morgan, P.; Stock, J. R.; Tsao, D. H. H.; Wissner, A.; Yang, X.; Chaudhary, D. *J. Med. Chem.* **2008**, *51*, 5958; (h) Cywin, C. L.; Dahmann, G.; Prokopowicz, A. S.; Young, E. R. R.; Magolda, R. L.; Cardozo, M. G.; Cogan, D. A.; DiSalvo, D.; Ginn, J. D.; Kashem, M. A.; Wolak, J. P.; Homon, C. A.; Farrell, T. M.; Grbic, H.; Hu, H.; Kaplita, P. V.; Liu, L. H.; Spero, D. M.; Jeanfavre, D. D.; O'Shea, K. M.; White, D. M.; Woska, J. R.; Brown, M. L. *Bioorg. Med. Chem. Lett.* **2007**, *17*(1), 225.
5. Xu, Z.; Chaudhary, D.; Olland, S.; Wolfrom, S.; Czerwinski, R.; Malakian, K.; Lin, L.; Stahl, M. L.; Joseph-McCarthy, D.; Benander, C.; Fitz, L.; Greco, R.; Somers, W. S.; Mosyak, L. *J. Biol. Chem.* **2004**, *48*, 50401.
6. Friesner, R. A.; Banks, J. L.; Murphy, R. B.; Halgren, T. A.; Klicic, J. J.; Mainz, D. T.; Repasky, M. P.; Knoll, E. H.; Shaw, D. E.; Shelley, M.; Perry, J. K.; Francis, P.; Shenkin, P. S. *J. Med. Chem.* **2004**, *47*(7), 1739.
7. (a) Van Eis, M. WO 2008/122614.; (b) For a detailed description of the PKC assays, see also Supplementary data.
8. Meredith, E. L.; Ardayfio, O.; Beattie, K.; Dobler, M. R.; Enyedy, I.; Gaul, C.; Hosagrahara, V.; Jewell, C.; Koch, K.; Lee, W.; Lehmann, H.; McKinsey, T. A.; Miranda, K.; Pagratis, N.; Pancost, M.; Patnaik, A.; Phan, D.; Plato, C.; Qian, M.; Rajaraman, V.; Rao, C.; Rozhitskaya, O.; Ruppen, T.; Shi, J.; Siska, S. J.; Springer, C.; van Eis, M. J.; Vega, R. B.; von Matt, A.; Yang, L.; Yoon, T.; Zhang, J.; Zhu, N.; Monovich, L. G. *J. Med. Chem.* **2010**, *53*(15), 5400.
9. Full experimental details and crystallographic data for the structure of **12** bound to PKXη have been deposited at the RCSB Protein Databank as PDB 3txo.
10. (a) Cywin, C. L.; Zhao, B.-P.; McNeil, D. W.; Hrapchak, M.; Prokopowicz, A. S.; Goldberg, D. R.; Morwick, T. M.; Gao, A.; Jakes, S.; Kashem, M.; Magolda, R. L.; Soll, R. M.; Player, M. R.; Bobko, M. A.; Rinker, J.; DesJarlais, R. L.; Winters, M. P. *Bioorg. Med. Chem. Lett.* **2003**, *13*, 1415; (b) Pierre, F.; Chua, P. C.; O'Brien, S. E.; Siddiqui-Jain, A.; Bourbon, P.; Haddach, M.; Michaux, J.; Nagasawa, J.; Schwaebe, M. K.; Stefan, E.; Vialettes, A.; Whitten, J. P.; Chen, T. K.; Darjania, L.; Stansfield, R.; Anderes, K.; Bliesath, J.; Drygin, D.; Ho, C.; Omori, M.; Proffitt, C.; Streiner, N.; Trent, K.; Rice, W. G.; Ryckman, D. M. *J. Med. Chem.* **2011**, *54*, 635.
11. For a description of the assay, see Supplementary data.
12. Upstate KinaseProfiler™.
13. High-throughput permeability assay: Wohnsand, F.; Faller, B. *J. Med. Chem.* **2001**, *44*, 923.
14. Measurement of plasma protein binding via rapid equilibrium dialysis: Waters, N. J.; Jones, R.; Williams, G.; Sohal, B. *J. Pharm. Sci.* **2008**, *97*, 4586.
15. Radioligand binding assay for hERG channel blockers: Finlayson, K.; Turnbull, L.; January, C. T.; Sharkey, J.; Kelly, J. S. *Eur. J. Pharmacol.* **2001**, *430*, 147.
16. For a description of the SEB model, see Supplementary data.
17. For the use of the SEB model in mice for testing immunosuppressive compounds, see: Kuschnaroff, L. M.; Valckx, D.; Goebels, J.; Rutgeerts, O.; Heremans, H.; Froyent, G.; Waer, M. *Scand. J. Immunol.* **1997**, *46*, 459.